Low energy range dielectronic recombination of Fluorine-like Fe^{17+} at the CSRm *

Nadir Khan[1,2] Zhong-Kui Huang(黄忠魁)[1] Wei-Qiang Wen(汶伟强)[1;1)] Sultan Mahmood[1]
Li-Jun Dou(豆丽君)[1,2] Shu-Xing Wang(汪书兴)[3] Xin Xu(许鑫)[3] Han-Bing Wang(汪寒冰)[1]
Chong-Yang Chen(陈重阳)[4] Xiao-Ya Chuai(啜晓亚)[1,2] Xiao-Long Zhu(朱小龙)[1] Dong-Mei Zhao(赵冬梅)[1]
Li-Jun Mao(冒立军)[1] Jie Li(李杰)[1] Da-Yu Yin(殷达钰)[1] Jian-Cheng Yang(杨建成)[1]
You-Jin Yuan(原有进)[1] Lin-Fan Zhu(朱林繁)[3] Xin-Wen Ma(马新文)[1;2)]

[1] Institute of Modern Physics, Chinese Academy of Sciences, Lanzhou 730000, China
[2] University of Chinese Academy of Sciences, Beijing 100049, China
[3] Hefei National Laboratory for Physical Sciences at Micro Scale,
Department of Modern Physics, University of Science and Technology of China, Hefei 230026, China
[4] Shanghai EBIT Laboratory, Key Laboratory of Nuclear Physics and Ion-beam Application, Institute of Modern Physics,
Department of Nuclear Science and Technology, Fudan University, Shanghai 200433, China

Abstract: The accuracy of dielectronic recombination (DR) data for astrophysics related ions plays a key role in astrophysical plasma modeling. The absolute DR rate coefficient of Fe^{17+} ions was measured at the main cooler storage ring at the Institute of Modern Physics, Lanzhou, China. The experimental electron-ion collision energy range covers the first Rydberg series up to $n = 24$ for the DR resonances associated with the $^2P_{1/2} \rightarrow {}^2P_{3/2}\Delta n = 0$ core excitations. A theoretical calculation was performed by using FAC code and compared with the measured DR rate coefficient. Overall reasonable agreement was found between the experimental results and calculations. Moreover, the plasma rate coefficient was deduced from the experimental DR rate coefficient and compared with the available results from the literature. At the low energy range, significant discrepancies were found, and the measured resonances challenge state-of-the-art theory at low collision energies.

Keywords: storage ring, electron cooler, electron-ion recombination, plasma rate coefficient

PACS: 34.80.Lx, 52.20.Fs **DOI:** 10.1088/1674-1137/42/6/064001

1 Introduction

Astrophysical plasmas can be divided into two broad classes: photoionized plasma and collisionally ionized plasma [1]. Photoionized plasma forms in the media surrounding cosmic sources such as active galactic nuclei (AGN), cataclysmic variable stars and X-ray binaries, where the ionization is because of photons [2]. However, collisionally ionized plasma is mostly found in solar coronae, supernova remnants, galaxies and in the intercluster medium in clusters of galaxies, where the ionization is by electron impact [3]. In order to understand the properties of astrophysical plasmas, a new generation of X-ray observatories, such as ASCA (JAXA) [4], Chandra (NASA) [5] and XMM-Newton (ESA) [6], have been launched to observe the high resolution X-ray spectra from various cosmic sources. All the observed spectra have to be interpreted by plasma modelling. However, most of the input atomic data for the plasma modeling are from theory. For electron-ion collision processes in astrophysical plasmas, dielectronic recombination (DR) is one of the important recombination processes, determining the charge state distribution and ionization balance. Therefore, precise DR rate coefficients are an issue of major concern for astrophysical plasma modeling [7–10]. In the case of collisionally ionized plasma, theoretical DR data are now available in the literature [3, 11, 12] with rather good agreement with the experimental data for plasma modeling [13]. To use this available atomic data for X-ray astrophysics implications, atomic databases such as XSPEC [14], AtomDB version 1.3 and AtomDB version 2.0 [15] are widely used to model astrophysical plasmas. However, for DR in photoionized plasma in the low-energy range, the modeling is mostly

Received 14 March 2018, Published online 11 May 2018

∗ Supported by the National Key R&D Program of China (2017YFA0402300), the National Natural Science Foundation of China through (11320101003, U1732133, 11611530684) and Key Research Program of Frontier Sciences, CAS (QYZDY-SSW-SLH006)

1) E-mail: wenweiqiang@impcas.ac.cn Corresponding author

2) E-mail: x.ma@impcas.ac.cn

based on theoretical predictions and calculations, and many theories cannot provide sufficiently precise DR rate coefficients [16]. In addition, the recent experimental approach for low energy range DR investigation has also shown that earlier computations of low temperature DR rate coefficients are not accurate [17–19]. To model the line emission, thermal and ionization structures of plasmas, astrophysicists require accurate benchmark atomic data from electron-ion recombination experiments [20].

Iron is the most abundant heavy element in astrophysical plasmas and is very important in astrophysics [9, 21]. High resolution X-ray spectra from $\sim$ 14 Å to $\sim$ 17 Å have been observed from different active galactic nuclei (AGN) such as the luminous quasar IRAS 13349+2438 [22] and Seyfert 1 galaxy NGC-3783 [23]. The rich absorption features contributed by iron ions have been seen in these spectra, when analyzed using photoionization codes CLOUDY [24] and XSTAR [25]. However, large discrepancies are found between the observed spectra and the results obtained from available DR theoretical data for iron ions. These discrepancies are due to underestimation of the low-temperature DR rate coefficient by available models for L-shell and M-shell iron ions. In order to solve this problem, electron-ion recombination experiments on different charge states of iron ions have been initiated at the test storage ring (TSR) [7, 26], Heidelberg Germany. The purpose was to provide accurate experimental DR data and reduce the uncertainties in calculations. For the case of F-like iron ions, most of the earlier calculations neglect the contribution from the fine structure $2p_{3/2}$–$2p_{1/2}$ excitations, which have been shown to be very important for the low-temperature DR rate coefficient [27]. Especially for photoionized plasma modeling, the inclusion of fine-structure excitation is very important for producing a reliable DR rate coefficient [26, 28, 29]. The other important astrophysical aspect of the fluorine-like ions forming neon-like ions is the determination of solar and stellar upper atmosphere abundances [30]. Here, we present absolute electron-ion recombination rate coefficients of fluorine-like Fe^{17+} from an experiment at the main cooler storage ring (CSRm) at the Institute of Modern Physics, Lanzhou, China, and also from a theoretical calculation using flexible atomic code (FAC) [31]. It should be noted that the electron-ion merged beams technique at heavy-ion cooler storage rings is the only laboratory method capable of studying DR at low collision energy. It also provides a high resolution with low background measurement of DR for precision atomic spectroscopy [19, 32, 33].

Dielectronic recombination is a two-step process, where one free electron is captured in one of the Rydberg states of the ion with simultaneous excitation of a core electron, producing a doubly excited intermediate state. This process completes when the system stabilizes itself to below ionization threshold by emitting excess energy in form of a photon. Another co-existing recombination process called radiative recombination (RR) also occurs at the same time. RR is the process where one free electron is captured into a bound state of the ion and a photon is emitted. For electron-ion recombination of F-like Fe^{17+}, RR can be expressed as

$$Fe^{17+}+e^- \rightarrow Fe^{16+}+h\nu \quad (1)$$

and DR for $\Delta n = 0$ transitions can be written as

$$Fe^{17+}(2s^22p^5[^2P_{3/2}])+e^- \rightarrow \begin{cases} Fe^{16+}(2s^22p^5[^2P_{1/2}]nl) & n=18,19...,\infty \\ Fe^{16+}(2s2p^6[^2S_{1/2}]nl) & n=6,7,...,\infty \end{cases}. \quad (2)$$

In the present recombination experiment of F-like iron, the experimental electron-ion collision energy range was 0−6 eV in the center of mass frame (c.m). It covers the first Rydberg series associated with the transition $^2P_{3/2} \rightarrow {}^2P_{1/2}$, where n is the principal quantum number and can be resolved up to $n = 24$.

The paper is organized as follows. Section 2 gives a brief introduction to the experimental method and data analysis. The experimental, calculated and plasma rate coefficients are presented and discussed in Section 3. A conclusion is given in Section 4.

2 Experimental method

The experiment was performed at the main cooler storage ring (CSRm), at the Institute of Modern Physics, Lanzhou, China [34]. Details about DR experiments at the CSRm have been described in Refs. [18, 35]. Here we just briefly describe the DR experiment of $^{56}Fe^{17+}$. The F-like Fe^{17+} ions were produced in the super-conducting Electron Cyclotron Resonance (ECR) ion source, and accelerated in the Sector Focused Cyclotron (SFC) up to an energy of $E_{\rm ion}$ = 6.08 MeV/u. After that, the ion beam was injected into the CSRm and stored in the ring. The storage lifetime of the ion beam was around 20 s. The beam current was $I_{\rm ion} \sim 350$ μA, corresponding to 2.3 $\times 10^8$ ions. The electron-cooler was employed to cool the ion beams and also used as an electron-target for the electron-ion recombination experiment. The electron beam was produced at the cathode and collected at the anode of the 35 kV electron cooler (EC-35). The magnetic fields applied at the cathode and cooler section were 1250 Gs and 390 Gs, respectively, allowing adiabatic expansion of the electron beam with expanded diameter of $d \sim 50$ mm.

The circulating ion beam merged with the electron beam to an effective length of 4 m in the electron cooler EC-35 at the CSRm. The mean velocity of the electron

beam was matched to the mean velocity of the ion beam at the cooling point. The detuning voltage $U_{\rm d}$ was applied to the cathode of the electron cooler to change the electrons' kinetic energy relative to the ions according to a specific time scheme *i.e.* 10 ms detuning and 190 ms of cooling [36]. The recombined ion beam was separated from the primary ion beam in the first dipole magnet downstream the electron cooler. Finally, the recombined Fe^{16+} ions were detected by a scintillator detector (YAP: Ce + PMT) with $\sim$ 100% efficiency [37]. During the whole measurement, a Schottky pick-up system was used to monitor the revolution frequency and longitudinal momentum spread of the ion beam. The momentum spread of the ion beam was deduced to be about $\Delta p/p\sim 3.4\times10^{-4}$ from the Schottky spectrum.

Data acquisition was started after 3 seconds of electron cooling following the beam injection. The electron-ion recombination rate coefficient can be determined from

$$\alpha(E)=\frac{R}{N_{\rm i}n_{\rm e}(1-\beta_{\rm e}\beta_{\rm i})}\cdot\frac{C}{L}, \tag{3}$$

where R is the count rate, $N_{\rm i}$ is the number of stored ions, $n_{\rm e}$ is the density of electron beam, $\beta_{\rm e}$ and $\beta_{\rm i}$ are the velocities of the electrons and ions respectively, C is the circumference of the ring, about 161.00 m, and L is length of the interaction region [35]. In order to obtain the recombination rate coefficient, the electron-ion collision energy from the laboratory frame system has to be transformed to the center-of-mass-frame (c.m.) system. To calculate the relative collision energy ($i.e.E_{\rm rel}$) between electrons and ions in the c.m. system, the following relativistic formula was used

$$E_{\rm rel} = \sqrt{m_{\rm e}^2c^4+m_{\rm i}^2c^4+2m_{\rm e}m_{\rm i}\gamma_{\rm e}\gamma_{\rm i}c^4(1-\beta_{\rm e}\beta_{\rm i}\cos\theta)} -m_{\rm e}c^2-m_{\rm i}c^2, \tag{4}$$

where $m_{\rm i}$ and $m_{\rm e}$ are the masses of ion and electron respectively. $\gamma_{\rm i}$, $\gamma_{\rm e}$ and $\beta_{\rm i}$, $\beta_{\rm e}$ are Lorentz factors and relativistic factors for ion beam and electron beam, respectively. $c$is the speed of light and θ is the angle between the ion and electron beams, which was always optimized to less than 0.1 mrad during measurement.

The space charge effect of the electron-beam was taken into account for calculating the relative collision energy, as the effective electron beam energy ($E_{\rm e}$) is

$$E_{\rm e}=-e(U_{\rm cath}+U_{\rm d}+U_{\rm sp}) \tag{5}$$

where $U_{\rm d}$ is the detuning voltage and $U_{\rm sp}$ is the space charge potential. The space-charge potential is modelled by the formula

$$U_{\rm sp}(v_{\rm e})=(1-\zeta)\frac{I_{\rm e}r_{\rm c}m_{\rm e}c^2}{v_{\rm e}e^2}\left[1+2\ln\left(\frac{b}{a}\right)-\left(\frac{r}{a}\right)^2\right]. \tag{6}$$

Here $I_{\rm e}$ is the electron beam current,$r_{\rm c}$ the classical electron radius, $m_{\rm e}$ is the electron rest mass, c is the speed of light, $v_{\rm e}$ is the electron velocity, e is the elementary charge, r is the distance from the electron beam axis, and $a=$ 2.8 cm and $b=$ 20 cm are the radii of the electron beam and the cooler tube, respectively. The parameter ζ accounts for the residual gas ions that are usually trapped in the electron beam. The calculated space-charge potential from the experimental parameters at cooling point was $U_{\rm sp}\sim$ 140 V.

3 Results and discussion

3.1 Electron-ion recombination rate coefficient

Figure 1 shows the electron-ion recombination rate coefficient as a function of electron-ion collision energy for F-like Fe^{17+} ions. The series associated with the $\Delta n=$ 0 core excitations from $2s^22p^5(^2P_{3/2})$ nl to $2s^22p^5(^2P_{1/2})$ nl were observed. The resonance positions were obtained from the Rydberg formula

$$E_{\rm res}=\Delta E-Ry\left(\frac{q}{n}\right)^2, \tag{7}$$

where $Ry=$ 13.606 eV is the Rydberg constant, $q=17$ is the charge state of the ion, and $\Delta E=$ 12.7182 eV is the core excitation energy taken from the NIST database [38]. The first Rydberg series of intermediate Fe^{16+} resonant states are identified from n=18 up to $n=24$.

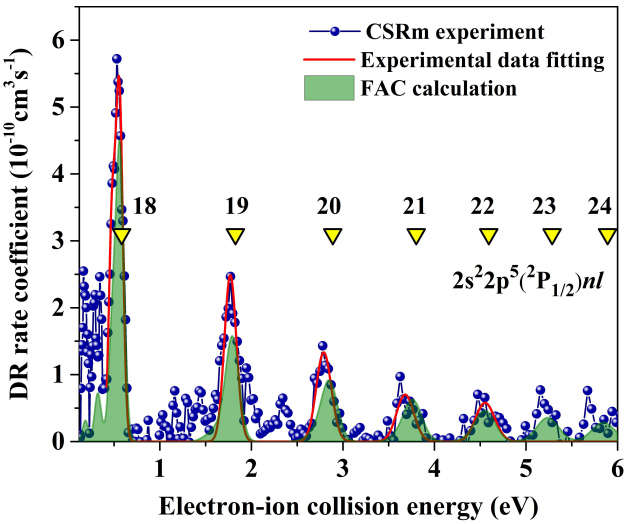

Fig. 1. (color online) Dielectronic recombination rate coefficient for Fe^{17+} ions from measurement (connected blue dots) are compared with a calculation based on FAC code (shaded green area). The yellow triangles indicate calculated Rydberg states associated with $^2P_{1/2}\rightarrow{}^2P_{3/2}$ core transitions. The solid red line shows the fitting result for obtaining the temperature of the measured DR rate coefficient at CSRm.

It should be noted that the recombination rate coefficient is obtained by convolution of resonance cross sections $\sigma_{\rm d}(v)$ with an asymmetrical Maxwell-Boltzmann

distribution function, resembling the distribution of relative velocities between the electrons and the circulating ions, *i.e.*

$$\alpha(E_{\rm rel})=\int\sigma(v)vf(\vec{v},v_{\rm rel})\mathrm{d}^3\vec{v}, \quad (8)$$

where $\sigma(v)$ is the energy-averaged cross section of the DR process. The theoretical cross section of state d is written as

$$\hat{\sigma}_{\rm d}(v)=\frac{2\pi\hbar Ry}{E_{\rm d}}\pi a_0^2\frac{g_{\rm d}}{2g_{\rm i}}\frac{A_a({\rm d}\to{\rm i})\sum\limits_{\rm f}A_r({\rm d}\to{\rm f})}{\sum\limits_{\rm k}A_a({\rm d}\to{\rm k})+\sum\limits_{\rm f'}A_r({\rm d}\to{\rm f'})}, \quad (9)$$

where $\hat{\sigma}_{\rm d}(v)$ is known as the strength of the resonance state d and is defined as the energy integrated cross section, Ry is the Rydberg constant, $E_{\rm d}$ is the resonance energy, and a_0 is the Bohr radius. $g_{\rm i}$ and $g_{\rm d}$ are the statistical weights of the initial ionic core and of the intermediate states, and A_a and A_r are autoionization and radiative decay rates, respectively. In summations k denotes all the states which are attainable by autoionization of the intermediate state, f runs over all states below the first ionization threshold, and f' includes all states below d [31, 32]. In Eq. (8), the $f(\vec{v},v_{\rm rel})$ is a flattened Maxwellian distribution function of the electron beam and is expressed by

$$f(\vec{v},v_{\rm rel}) = \frac{m_{\rm e}}{2\pi k_{\rm B}T_\perp}\exp\left(-\frac{m_{\rm e}v_\perp^2}{2k_{\rm B}T_\perp}\right)\times\left[\frac{m_{\rm e}}{2\pi k_{\rm B}T_\parallel}\right]^{1/2} \times\exp\left(-\frac{m_{\rm e}(v_\parallel-v_{\rm rel})^2}{2\pi k_{\rm B}T_\parallel}\right), \quad (10)$$

where $m_{\rm e}$ is the mass of the electron, $k_{\rm B}$ is the Boltzmann constant, and $T_\perp$ and $T_\parallel$ are the experimental electron velocity distributions of the parallel and perpendicular temperatures respectively, with respect to the electron beam propagation direction. $v_{\rm rel}$ is the relative velocity between electron and ion [39].

The measured DR spectrum from 0.38 eV up to 5 eV is fitted with six resonances associated with $2s^22p^5(^2P_{1/2})$ nl, where n = 18, 19, 20, 21, 22. The resonance energies and strengths obtained are listed in Table 1. The electron beam temperatures obtained from this fitting are $K_{\rm B}T_\parallel$=1.2 meV and $K_{\rm B}T_\perp$=11 meV. The energy resolution achieved was less than $\Delta E\sim 0.09$ eV at full width at half maximum (FWHM) around $E_{\rm rel}\sim$ 0.49 eV.

The uncertainty of the experimental recombination rate coefficient is estimated to be about 30%, an uncertainty of 10% due to a combination of counting statistics, electron and ion beam currents, and interaction length, and an uncertainty of 20% due to the electron density distribution profile and also the position of the ion beam in this profile.

The theoretical calculations were performed by using FAC code [40]. The doubly excited states $2s^22p^5[^2P_{1/2}]\,nl$, $n=18\sim24$ of Ne-like Fe^{16+} ions were included. Here the l values went up to $l_{\rm max}$=20. For the Fe^{17+} ions, all possible electronic-dipole transitions from the $2s^22p^5[^2P_{1/2}]nl$ resonances were considered. The theoretical rate coefficient was obtained by convoluting the calculated resonance cross sections with the experimental electron energy distribution (see Eq. (8)). The calculated DR rate coefficient is shown by the green area in Fig. 1. The measured rate coefficient and the theoretical calculation are in reasonable good agreement. However, the theory is slightly lower than the experiment in the low energy range. This means that the calculated result by FAC code cannot reproduce the DR rate coefficient both in energy positions and intensities comparable to the measured results in the very low energy range. These discrepancies are associated with the DR resonances Fe^{16+} $2s^22p^5(^2P_{1/2})nl$, where n=18$\sim$ 24.

Table 1. Resonance energies and strengths from the fitted DR resonances of the measured recombination rate coefficient from 0.18 to 5 eV (see graph fitting in Fig. 1). The numbers in parenthesis represent the uncertainties.

$E_{\rm d}$/eV	$\sigma_{\rm d}/(10^{-21}{\rm cm}^2/{\rm eV})$
0.19 (0.03)	588 (39)
0.33 (0.03)	517 (39)
0.49 (0.04)	704 (54)
0.57 (0.04)	1093 (54)
1.79 (0.07)	521 (38)
2.81 (0.09)	278 (38)
3.70 (0.10)	146 (39)
4.57 (0.11)	121 (39)

The n-sum resonance strengths derived from the experimental data for energy range of 0.38 eV−5 eV are compared with the experimental data from TSR storage ring [13] as shown in Table 2. In addition, the calculated strengths by FAC code (this work), and the previously calculated results by the state-of-the-art codes Multi-Configuration Dirac Fock (MCDF) and multi-configuration Breit-Pauli (MCBP) are also shown in Table 2. Because of the statistical uncertainty in experimental measurement below 0.38 eV, the first two peaks related to 18s and 18p were not measured accurately, so the n = 18l value was only considered for 18d and 18l with $l\geqslant3$ peaks for all the data under comparison. A good agreement between our data and TSR data can be found for the resonance strengths of n=18$\sim$ 22. This comparison shows that CSRm can also provide reliable experimental data to benchmark theory for astrophysical plasma modeling and for precision spectroscopic investigation. However, Table 2 shows a clear difference between the measured and calculated DR resonance strengths and also slight differences between differ-

Table 2. Resonance strengths of the first five DR resonances from this work (measurement at CSRm and FAC calculations) and from previous work (measurement at TSR and MCDF, MCBP calculations) for Δn= 0 [13, 41]. Here $\sigma_{\rm d}$ represents the energy-integrated cross sections for $2s^22p^5(^2P_{1/2})nl$ resonances.

n	$\hat{\sigma}_{\rm d}/(10^{-21}{\rm cm}^2{\rm eV})$				
	CSRm (experiment)	TSR (experiment)	FAC (this work)	MCDF	MCBP
18	1797 (77)	2018 (13)	1417.5	1557.4	1634.5
19	521 (38)	606 (14)	427.1	449.7	477.6
20	278 (38)	336.5 (8.6)	227.4	239.7	252.2
21	146 (39)	205.4 (6.9)	149.1	154.5	161.1
22	121 (39)	140.7 (4.2)	105.5	111.1	113.2

Note: In this table the strengths for sum of n= 18l value does not include the contribution from 18s and 18p. For more details see text.

ent theoretical calculations. Further precise experimental results and also theories of the DR rate coefficients for highly charged ions are required.

3.2 Plasma rate coefficient

The plasma rate coefficient, which is useful for astrophysical plasma modelling, can be obtained by convoluting the recombination rate coefficient with the Maxwell-Boltzmann energy distribution of the electrons in a plasma as [42, 43]

$$\alpha(T_{\rm e})=\int\alpha(E)f(E,T_{\rm e}){\rm d}E, \tag{11}$$

where the term $\alpha(E)$ represents the measured electron-ion recombination rate coefficient and $f(E,T_{\rm e})$ is the average Maxwellian temperature distribution function as given by

$$f(E,T_{\rm e})=\frac{2E^{1/2}}{\pi^{1/2}(k_{\rm B}T_{\rm e})^{3/2}}\exp\left(-\frac{E}{k_{\rm B}T_{\rm e}}\right), \tag{12}$$

where E is the relative energy and $T_{\rm e}$ is the electron temperature.

As shown in Fig. 2, the plasma rate coefficient for DR in Fe^{17+} was deduced from the measured electron-ion recombination rate coefficient in the temperature range from 0.1 eV to 4.7 eV. The values of strengths and energy positions were used to obtain the plasma rate coefficient, which were extracted from fitting the DR rate coefficient and compared with the calculated data from FAC code and also from the literature. The plasma rate coefficients derived from the measurement at the CSRm and FAC calculation are shown by the thick blue solid and thin green solid lines, respectively. The previous results from the measurement at the TSR are indicated by the purple dash-dotted line, and the corresponding theoretical calculations by using MCBP and MCDF are denoted by the red dashed-dot-dot curve and black dotted curve, respectively. At temperatures from 0.1 eV to 1.0 eV the theoretical calculations from FAC are $\sim$ 30% lower than the CSRm experimental results. At this low energy range the discrepancies can also be interpreted as from change of resonance positions, because the plasma rate coefficient is very sensitive to changes in resonance positions and strengths in the merged beam recombination rate coefficient in the low energy range. A small change in position and strengths translate into large discrepancies in plasma rate coefficient [17]. However, in the temperature range from 2.0 eV to 4.7 eV, a very good agreement is found between experimental results and FAC calculation. The plasma rate coefficient from CSRm agrees very well with the TSR data from 0.1 eV to 0.3 eV, and is about $\sim$ 20% lower than the TSR data from 0.5 eV to 4.7 eV. It can be found that the MCDF and MCBP

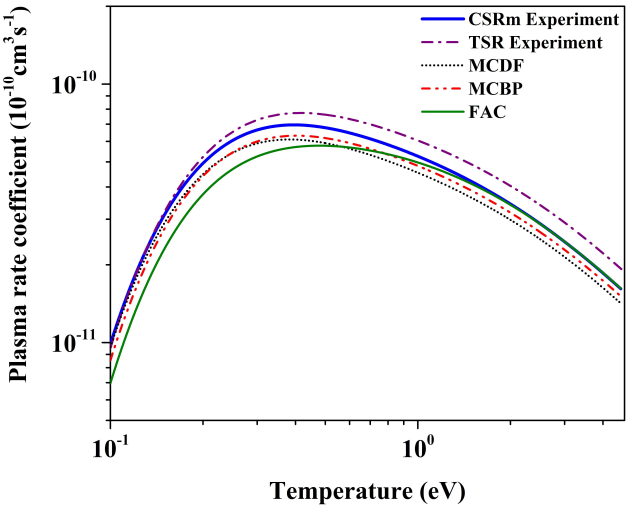

Fig. 2. (color online) Comparison of plasma rate coefficient derived from experimental results with the calculated results from FAC code and the existing plasma rates coefficients from the literature. The plasma rate is derived from 18 $\sim$ 22 resonance strengths. The contributions from 18s and 18p are not taken into account, as indicated in Table 2. The thick solid blue line denotes experimental results from CSRm and the thin solid green line represents the FAC calculation. The experimental results from TSR are displayed by the purple dash-dotted line and the corresponding calculations by MCBP and MCDF are shown by the red dashed curve and black dotted curve, respectively. Since our measurement energy range is only up to 5 eV and the contribution from 18s and 18p are missing in this figure, this plasma rate cannot be used in plasma modeling.

results underestimate the plasma rate coefficient in this temperature range, and clear discrepancies can be seen in the plasma rate coefficient measured by TSR (dash-dotted line) and all the theoretical calculations. In the temperature range of 0.2 eV to 4.7 eV all the calculations underestimate the plasma rate coefficient by about 30% as compared with the TSR. These discrepancies show that calculation of accurate DR resonance structure at low energy collisions is still a very challenging task even for state-of-the-art codes.

4 Conclusions

The DR rate coefficient of F-like iron in the energy range 0−6 eV has been measured by employing the electron-ion merged beams method at the CSRm at Lanzhou, China. The measured energy range covers the first Rydberg series of $^2P_{1/2}$ to $^2P_{3/2}$core transitions of Δn= 0 up to n= 24. A FAC code was employed to calculate the DR rate coefficient to compare with the measured results. A reasonably good agreement between the experimental results and the calculations could be found by taking into account the estimated 30% experimental uncertainty. The plasma rate coefficient derived from the electron-ion recombination rate coefficient was compared with the FAC calculation and also the available data in the literature, and overall a reasonable agreement was found. However, discrepancies between experimental and theoretical results can be seen in the low temperature range, which can be mainly attributed to the limited accuracy of the theoretical calculation. Our measurement challenges modern DR theory to calculate accurate electron-ion recombination rate coefficients of multi-electron ions at low electron-ion collision energies.

Nadir Khan acknowledges the China Scholarship Council (CSC) of China for providing opportunity and funding for him to study at IMP, UCAS. W. Wen thanks the Youth Innovation Promotion Association CAS for their support. We would like to thank Daniel Wolf Savin for providing his data on the internet and Stefan Schippers for guiding us in the data analysis. The authors would like to thank the crew of the Accelerator Department for skillful operation of the CSR accelerator complex.

References

1 D. W. Savin, AIP Conference Proceedings, **926**: 124 (2007)
2 T. R. Kallman, Space Sci. Rev., **157**: 177 (2010)
3 P. Bryans et al, Astrophys. J. suppl. S., **167**: 343 (2006)
4 C. S. Reynolds, A. Fabian, Mon. Not. R. Astron. Soc., **273**: 1167 (1995)
5 M. C. Weisskopf et al, X-Ray Optics, Instruments, and Missions III, **4012**: 2 (2000)
6 F. Jansen et al, A&A, **365**: L1 (2001)
7 D. W. Savin, AIP Conference Proceedings, **774**: 297 (2005)
8 A. Müler, Adv. Atom. Mol. Opt. Phys., **55**: 293 (2008)
9 S. Schippers et al, Int, Rev. At. Mol. Phys., **1**: 109 (2010)
10 O. Novotn et al, Astrophys. J., **753**: 57 (2012)
11 P. Mazzotta et al, Astron. Astrophys. Suppl. S., **133**: 403 (1998)
12 P. Bryans, E. Landi, D. W. Savin, Astrophys. J., **691**: 1540 (2009)
13 D. W. Savin et al, Astrophys. J. suppl. S., **123**: 687 (1999)
14 K. Arnaud, Astronomical Data Analysis Software and Systems V, **101**: 17 (1996)
15 R. K. Smith et al, Astrophys. J. Lett., **556**: L91 (2001)
16 T. Kallman, P. Palmeri, Rev. Mod. Phys., **79**: 79 (2007)
17 S. Schippers et al, Astron. Astrophys., **421**: 1185 (2004)
18 Z. Huang et al, Astrophys. J. suppl. S., **235**: 2 (2018)
19 S. Mahmood et al, Astrophys. J., **771**: 78 (2013)
20 N. R. Badnell, J. Phys. B: at. Mol. Opt., **39**: 4825 (2006)
21 S. Schippers et al, J. Phys.: Conf. Ser., **388**: 062029 (2012)
22 M. Sako et al, Astron. Astrophys., **365**: L168 (2001)
23 H. Netzer et al, Astrophys. J., **599**: 933 (2003)
24 G. Ferland et al, Publ. Astron. Soc. Pac., **110**: 761 (1998)
25 T. Kallman et al, Astrophys. J. suppl. S., **155**: 675 (2004)
26 S. Schippers et al, J. Phys.: Conf. Ser., **388**: 062029 (2012)
27 D. W. Savin et al, Astrophys. J. Lett., **489**: L115 (1997)
28 D. Savin et al, Astrophys. J., **642**: 1275 (2006)
29 G. J. Ferland, Annu. Rev. Astron. Astr., **41**: 517 (2003)
30 D. W. Savin, J. M. Laming, Astrophys. J., **566**: 1166 (2002)
31 M. F. Gu, Can. J. Phys., **86**: 675 (2008)
32 D. Bernhardt et al, Phys. Rev. A, **91**: 012710 (2015)
33 M. Lestinsky et al, Phys. Rev. Lett., **100**: 033001 (2008)
34 J.-W. Xia et al, Nucl. Instrum. Meth. A, **488**: 11 (2002)
35 Z. Huang et al, Phys. Scripta., **2015**: 014023 (2015)
36 M. Ling-Jie et al, Chinese Physics C, **37**: 017004 (2013)
37 W. Wen et al, Nucl. Instrum. Meth. B, **317**: 731 (2013)
38 T. Shirai et al, J. Phys. Chem. Ref. Data, **19**: 127 (1990)
39 S. Schippers et al, Phys. Rev. A, **62**: 022708 (2000)
40 C.-Y. Chen et al, J. Quant. Spectrosc. Ra, **111**: 843 (2010)
41 O. Zatsarinny et al, Astron. Astrophys., **447**: 379 (2006)
42 A. Müler, Int. J. Mass. Spectrom., **192**: 9 (1999)
43 M. Fogle et al, Astron. Astrophy., **409**: 781 (2003)